

In-plane anisotropy of the electron lifetime in the cuprates

R. Hlubina

Solid State Physics, Comenius University, Mlynská Dolina F2, 842 15 Bratislava, Slovakia

(Received 21 April 1998)

Nonlinear conductivity, skin effect, and transport across a barrier are proposed as experiments for a direct study of in-plane anisotropy of the electron lifetime in the cuprates. The magnitude of these effects within the recently proposed cold-spot model of the normal state of the cuprates is estimated. A modification of the cold-spot model yielding magnetotransport in agreement with experiments is proposed.
[S0163-1829(98)05337-5]

Transport properties of the normal state of high-temperature superconductors remain controversial. One school of thought ascribes them to the breakdown of Landau's Fermi-liquid theory.¹⁻³ In other types of theories the in-plane anisotropy of electron dynamics is considered to be crucial.^{4,5} Photoemission experiments⁶ have been cited as evidence for the latter point of view. However, the interpretation of photoemission spectra is still an open subject. Moreover, photoemission measures only the single-particle correlation function.⁶ In this paper we look for independent direct tests of anisotropy of the electron lifetime, τ . The microscopic origin of this anisotropy is irrelevant for our discussion, as long as there is a finite quasiparticle residue along the whole Fermi surface, which we assume. We consider only optimally doped materials. Numerical results are calculated within the cold-spot model,⁵ but we expect similar effects also for the model proposed in Ref. 4.

Cold-spot model. Ioffe and Millis⁵ assume that the two-dimensional (2D) Fermi line can be decomposed into segments which are "cold" and "hot," respectively. The hot segments occupy the majority of the Fermi line and are characterized by a large scattering rate Γ independent of temperature T . The four cold segments are located in the $[\pm 1, \pm 1]$ directions of the Fermi line (x and y are the directions of the Cu-O-Cu bond) and they exhibit a Fermi-liquid scattering rate $\hbar/\tau_0 = T^2/E_0$ with a characteristic energy E_0 . Let φ be the polar angle measured from the x axis. It is assumed⁵ that $\tau = \tau_0/[1 + (2\varphi_0)^{-2}\cos^2\varphi]$, where $\varphi_0 = (\hbar/4\tau_0\Gamma)^{1/2} \propto T$ is the angular size of a cold spot. Note that the criterion⁷ that anomalous scattering be generic on the Fermi line in order to imply anomalous transport at low T is satisfied in the cold-spot model.

Standard transport theory. In what follows, we consider single-layer tetragonal compounds such as $\text{Ti}_2\text{Ba}_2\text{CuO}_{6+\delta}$ with the c -axis lattice constant a_\perp . In order to simplify the analysis, we assume a cylindrical Fermi surface slightly modulated in the z direction. The in-plane dispersion is $\varepsilon_{\mathbf{k}} = \hbar^2 k^2/2m$, the average Fermi momentum and velocity are $\hbar k_F$ and $v_F = \hbar k_F/m$, respectively. In this case, standard transport theory⁸ predicts that the in-plane conductivity, Hall conductivity, and magnetoconductivity in a magnetic field $\mathbf{B}||z$ are $\sigma = \sigma_0 k_F v_F \langle \tau \rangle$, $\sigma_H/\sigma = \omega_c \langle \tau^2 \rangle / \langle \tau \rangle$, and $\Delta\sigma/\sigma = -\omega_c^2 \langle \tau^3 + \tau(\tau')^2 \rangle / \langle \tau \rangle$, respectively. $\omega_c = eB/m$ is the cyclotron frequency, $\sigma_0 = e^2/ha_\perp$, the angular average is de-

finied as $\langle A \rangle = \int_0^{2\pi} (d\varphi/2\pi) A(\varphi)$, and $\tau' = d\tau/d\varphi$. This implies for the cold-spot model $\sigma \propto \tau_0 \varphi_0 \propto T^{-1}$, $\sigma_H \propto \tau_0^2 \varphi_0 \propto T^{-3}$, and if one neglects the derivative term, $\Delta\sigma \propto \tau_0^3 \varphi_0 \propto T^{-5}$, in agreement with experiment.⁹ φ_0 can be thought of as a T -dependent carrier density and the cold-spot model resembles the transport phenomenology of Ref. 10. The Hall number $R_H = (a_\perp/n_\square|e|) \langle \tau^2 \rangle / \langle \tau \rangle^2$ is hole-like for a Fermi line centered around (π, π) , n_\square is the 2D density of unoccupied states. R_H saturates for $T \approx T^* \approx \pi/2 \sqrt{E_0 \Gamma}$ to $a_\perp/n_\square|e|$. For $\Gamma \approx 0.15$ eV and $E_0 \approx 12$ meV (Ref. 5) we estimate $T^* \approx 0.06$ eV. Unfortunately, the derivative term in $\Delta\sigma$ spoils the agreement with experiment, since it yields $\Delta\sigma \propto \tau_0^3/\varphi_0 \propto T^{-7}$. In the Appendix, we present a modification of the cold-spot model which produces σ , σ_H , and $\Delta\sigma$ in agreement with experiments.

Magnetoconductance. If $B \perp z$, the in-plane anisotropy of τ should be directly visible in magnetoconductance experiments. Such measurements with the current $j||z$ have been reported recently on overdoped $\text{Ti}_2\text{Ba}_2\text{CuO}_{6+\delta}$.¹¹ In that geometry, we can calculate the magnetoconductivity σ_{zz} to quadratic order in the (small) c -axis velocity $v_z = w(\varphi) \sin k_z a_\perp$ simply neglecting the c -axis warping of the cylindrical Fermi surface.¹² We find

$$\sigma_{zz} = \sigma_0 \frac{k_F}{v_F} \left\langle \frac{w^2 \tau}{1 + \Omega^2 \tau^2 \sin^2(\varphi - \chi)} \right\rangle, \quad (1)$$

where χ is the angle between B and x and $\Omega = eBv_F a_\perp/\hbar$ is the c -axis cyclotron frequency.¹² Since σ_{xz}, σ_{yz} are at least of order w^2 , $\rho_{zz} = 1/\sigma_{zz}$. We write $\rho_{zz} = \rho_{zz}^{(0)} + \rho_{zz}^{(2)} + \rho_{zz}^{(4)} + \dots$, where $\rho_{zz}^{(n)} \propto B^n$, and find $\rho_{zz}^{(2)}/\rho_{zz}^{(0)} = \frac{1}{2} \Omega^2 \langle w^2 \tau^3 \rangle / \langle w^2 \tau \rangle$ and $\rho_{zz}^{(4)}/\rho_{zz}^{(0)} = (\rho_{zz}^{(2)}/\rho_{zz}^{(0)})^2 - \Omega^4 \langle w^2 \tau^5 \sin^4(\varphi - \chi) \rangle / \langle w^2 \tau \rangle$. The lowest order (in B) anisotropic contribution is $\rho_{zz}^{(4)}$, in agreement with experiments. Unfortunately, besides $\tau(\varphi)$, also $w(\varphi)$ contributes to the anisotropy of $\rho_{zz}^{(4)}$. $w(\varphi)$ is expected to be small¹³ in the $[\pm 1, \pm 1]$ directions and this might be the cause of the observation¹¹ that the measured anisotropy of $\Delta\rho_{zz}/\rho_{zz}$ is not sufficiently large in order to explain the in-plane magnetotransport data.

Nonlinear conductivity. In order to observe the in-plane anisotropy of τ in a conductivity measurement, the symmetry of the plane has to be reduced. This is done by the action of the B field in magnetoconductance experiments and the same

effect is achieved in the nonlinear conductivity by the electric field $\mathbf{E}=(E_x, E_y, 0)$ itself. The symmetry of the problem implies

$$j_x = \sigma E_x + (\sigma_1 E_x^2 + \sigma_2 E_y^2) E_x,$$

$$j_y = \sigma E_y + (\sigma_2 E_x^2 + \sigma_1 E_y^2) E_y.$$

The nonlinear conductivities $\sigma_{1,2}$ can be found by the method of Jones and Zener⁸ from $j_\mu = 2e^2 \sum_{\mathbf{k}} \delta(\varepsilon_{\mathbf{k}} - \mu) v_{\mathbf{k}}^\mu (1 + \hat{A})^{-1} [\mathbf{E} \cdot \mathbf{v}_{\mathbf{k}} \tau_{\mathbf{k}}]$, where μ is the chemical potential and $\hat{A} = (e \tau_{\mathbf{k}} \mathbf{E} / \hbar) \cdot \partial / \partial \mathbf{k}$. Let us assume that $\partial \tau / \partial \varepsilon = 0$ at the Fermi surface. Then we find, under the assumption that transport is dominated by the directions $[\pm 1, \pm 1]$,

$$\sigma_1 = \frac{e^4}{4\pi m \hbar^2 a_\perp} \left\langle -\tau(\tau')^2 + \tau^2 \frac{\partial^2 \tau}{\partial v^2} \right\rangle,$$

$$\sigma_2 = \frac{e^4}{4\pi m \hbar^2 a_\perp} \left\langle \tau(\tau')^2 + 3\tau^2 \frac{\partial^2 \tau}{\partial v^2} \right\rangle,$$

where $v = \varepsilon / 2\mu$. Note a difference with respect to magnetotransport: nonlinear conductivity is a function not only of the angular dependence of τ but also of its energy dependence. This is because, unlike the B field, the electric field ‘heats’ the carriers. From a measurement of the nonlinear conductivity in two nonequivalent directions (say, $[100]$ and $[110]$), one can determine $\sigma_{1,2}$.

Let us assume first that the angular dependence of τ dominates. In this case $\sigma_2 = -\sigma_1 = \sigma / E_c^2$ and the cold-spot model predicts that the characteristic field is $E_c = (8/\sqrt{5}) \hbar \delta k / e \tau_0$, with $\delta k = \varphi_0 k_F$ the dimension of the cold spot. Using $k_F \approx 0.6 \text{ \AA}^{-1}$,⁵ we estimate for YBCO₇ at $T = 100 \text{ K}$ $E_c \approx 1.2 \times 10^7 \text{ V/m}$.

If the energy dependence of τ is dominant, the cold-spot model predicts $\sigma_2 = 3\sigma_1$. As developed in Ref. 5 the model does not specify the form of $\tau(\varepsilon)$. Assuming Fermi-liquid-like properties around cold spots, we take

$$\hbar / \tau_0 = [\varepsilon^2 + (\pi T)^2] / \pi^2 E_0. \quad (2)$$

This implies $\sigma_1 = -\sigma / E_c^2$ with $E_c = (4\pi / \sqrt{5}) (\sqrt{\Gamma E_0} / \mu) \hbar \delta k / e \tau_0$. Because of the factor $\sqrt{\Gamma E_0} / \mu$, the energy dependence of τ dominates over the angular one if Eq. (2) applies. At $T = 100 \text{ K}$ with $\hbar v_F \approx 1.3 \text{ eV \AA}$,¹⁴ we estimate $E_c \approx 2 \times 10^6 \text{ V/m}$.

Skin effect. The surface of the sample breaks the symmetry of the bulk and allows (in principle) for a different determination of the anisotropy of the in-plane lifetime. The impedance of a surface in a high-symmetry direction ($[100]$ or $[110]$) for an electromagnetic wave of frequency ω with the electric field polarized in the xy plane is¹⁵

$$Z = -\frac{i\mu_0\omega}{\pi} \int_{-\infty}^{\infty} \frac{dq}{-iq^2 - \omega^2/c^2 - i\omega\mu_0\sigma_\perp(q, \omega)},$$

where μ_0 is the permeability of vacuum and $\sigma_\perp(q, \omega)$ is the in-plane conductivity along the surface for a wave vector q perpendicular to the surface. For $\Gamma \gg \hbar\omega, \hbar q v_F$ the cold-spot model predicts

$$\sigma_\perp(q, \omega)^{[100]} = \frac{\sigma}{2} \left[\frac{1}{\sqrt{1 - i\tau_0\omega_+}} + \frac{1}{\sqrt{1 - i\tau_0\omega_-}} \right],$$

$$\sigma_\perp(q, \omega)^{[110]} = \frac{\sigma}{\sqrt{1 - i\tau_0\omega + (v_F q \tau_0 \varphi_0 / 2)^2}}, \quad (3)$$

for $q \parallel [100]$ and $q \parallel [110]$, respectively, where we have introduced $\omega_\pm = \omega \pm v_F q / \sqrt{2}$. Therefore the surface impedance depends on the surface orientation. Unfortunately, the effect is small. Indeed, the surface impedance $Z \propto 1/q_0$ where q_0 is the characteristic wavelength: $q_0^2 \approx \omega \mu_0 \sigma_\perp$. The relative change of Z between $[100]$ and $[110]$ surfaces $\delta Z / Z$ is proportional to the relative change of the corresponding conductivities $\delta \sigma_\perp / \sigma_\perp$. From Eq. (3) it follows that $\delta \sigma_\perp / \sigma_\perp \sim (v_F q_0 \tau_0)^2 < v_F^2 \tau_0 \mu_0 \sigma$. Taking $\sigma \sim 10^6 (\Omega \text{ m})^{-1}$,¹⁶ we estimate $\delta \sigma_\perp / \sigma_\perp < 4 \times 10^{-3}$.

The criterion for the appearance of an anomalous skin effect in the usual metals is $l \gg c / \omega_p$ where c is the speed of light, l is the electron mean free path, and ω_p is the plasma frequency. In the cuprates, both l and ω_p are smaller than in pure elemental metals and therefore the small anisotropy of the skin effect is not surprising. On the other hand, the condition $\omega \ll v_F q$ is automatically satisfied in experiments on ultrasound absorption. Unfortunately, since the anisotropy in Eq. (3) is well developed only for $q v_F \tau_0 \sim 1$, ultrasound with frequencies $\omega \sim v_s / (v_F \tau_0)$ is needed. For electronic parameters of YBCO₇ at $T = 100 \text{ K}$ we find, using a typical sound velocity¹⁷ $v_s \approx 4 \times 10^3 \text{ m/s}$, $\omega \approx 200 \text{ GHz}$. A neutron-scattering study of the angular dependence of the phonon linewidth might be useful.

Transport across a barrier. Consider a current flowing in the xy plane and a barrier perpendicular to the current flow. Let us denote the coordinate parallel (perpendicular) to the direction of the current as ξ (η). Electrons incident on the barrier ($v_{\mathbf{k}}^\xi > 0$) from the left piece of the metal (1) are described by the shifted Fermi distribution function $f_{1,\mathbf{k}} = f^0(\varepsilon_{\mathbf{k}} - eE\tau_{\mathbf{k}}v_{\mathbf{k}}^\xi)$, where E is the electric field in the electrodes.¹⁸ Similarly, electrons with $v_{\mathbf{k}}^\xi < 0$ in the right piece (2) are distributed according to $f_{2,\mathbf{k}} = f^0(\varepsilon_{\mathbf{k}} - eE\tau_{\mathbf{k}}v_{\mathbf{k}}^\xi + e\delta V)$, where δV is the voltage jump on the barrier. We assume a translationally invariant barrier in the η direction. Conservation of momentum and energy in the process of scattering of an electron on the barrier implies that a state $\mathbf{k} = (k_\xi, k_\eta)$ scatters either to the same state on the other side of the barrier or into $\mathbf{k}^* = (-k_\xi, k_\eta)$ on the same side. We consider only barriers in high-symmetry directions of the lattice, so that \mathbf{k}^* is symmetry equivalent to \mathbf{k} . The barrier is fully described by the probabilities of transition and reflection of a given state $\mathcal{T}_{\mathbf{k}}$ and $\mathcal{R}_{\mathbf{k}}$, respectively, with $\mathcal{T}_{\mathbf{k}} + \mathcal{R}_{\mathbf{k}} = 1$. Close to the barrier, the distribution function of the electrons in 2 with $v_{\mathbf{k}}^\xi > 0$ is $f_{2,\mathbf{k}} = \mathcal{T}_{\mathbf{k}} f_{1,\mathbf{k}} + \mathcal{R}_{\mathbf{k}} f_{2,\mathbf{k}^*}$.¹⁹ Similarly, electrons in 1 with $v_{\mathbf{k}}^\xi < 0$ obey $f_{1,\mathbf{k}} = \mathcal{T}_{\mathbf{k}} f_{2,\mathbf{k}} + \mathcal{R}_{\mathbf{k}} f_{1,\mathbf{k}^*}$. The current density across the barrier is $j = \sigma_0 (k_F / v_F) \langle [\delta V + 2E\tau_{\mathbf{k}} |v_{\mathbf{k}}^\xi|] |v_{\mathbf{k}}^\xi| \mathcal{T}_{\mathbf{k}} \rangle$. On the other hand, the current density in the electrodes is $j = \sigma_0 (k_F / v_F) \langle 2E\tau_{\mathbf{k}} (v_{\mathbf{k}}^\xi)^2 \rangle$. By comparing the two expressions for j we can determine δV . The resistivity per unit area of the barrier $\delta R_\square = \delta V / j$ is therefore

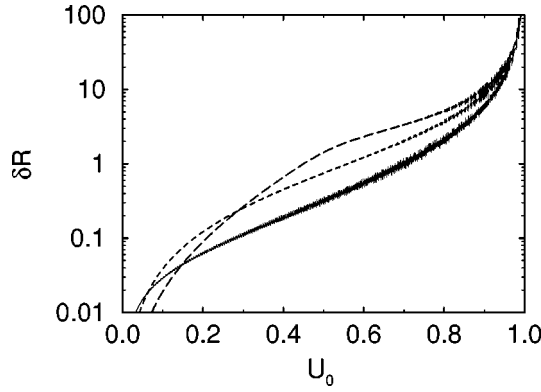


FIG. 1. δR_{\square} in units of $(\sigma_0 k_F)^{-1}$ as a function of the barrier height U_0 (in units of μ) for a barrier with $k_F d = 10^3$. The direction of the current flow is [100] (dashed line) and [110] (solid line). The angular dimension of the cold spot is $\varphi_0 = 0.1$. Short-dashed line: δR_{\square} for $\tau = \text{const}$.

$$\delta R_{\square} = \frac{1}{\sigma_0 k_F} \frac{2 \langle \cos^2 \theta \tau(\theta) \mathcal{R}(\theta) \rangle}{\langle \tau(\theta) \rangle \langle |\cos(\theta)| [1 - \mathcal{R}(\theta)] \rangle}, \quad (4)$$

where θ is the angle between \mathbf{k} and the ξ axis.²⁰ In the tunnel limit $\mathcal{R} \rightarrow 1$ Eq. (4) reduces to the well-known formula for the conductivity of a tunnel junction, $G_{\square} = \sigma_0 k_F \langle |\cos(\theta)| \mathcal{T}(\theta) \rangle$ which is independent of τ . The limit of a small barrier is more interesting. First, let us note that $\mathcal{R}(\pi/2) = 1$ for any nonvanishing barrier. With increasing barrier “strength,” the angular region around $\pm \pi/2$ where $\mathcal{R} \approx 1$ grows, leading to an increase of δR_{\square} . This enables us to measure the angular dependence of the electron lifetime.

To illustrate the point, let us consider a rectangular barrier with height $U_0 = \hbar^2 k_0^2 / 2m$ and width d . For a thick barrier $k_0 d \gg 1$, $\mathcal{R} \approx 1$ for $k_{\xi} < k_0$, while $\mathcal{R} \approx 0$ for $k_{\xi} > k_0$. Thus the angular integral in the numerator of Eq. (4) is dominated by $|\theta| > \theta_0$, where $\cos \theta_0 = k_0 / k_F$. Consider a variation of U_0 .²¹ For the current flowing in the [100] direction δR_{\square} grows with increasing U_0 until $\theta_0 \approx \pi/4$, when also the cold spots enter the region $\mathcal{R} \approx 1$. This happens for $U_0 \approx \mu/2$. For $U_0 > \mu/2$ the growth of δR_{\square} is predominantly due to the angular integral in the denominator of Eq. (4). At $U_0 \approx \mu$, $\mathcal{R} \approx 1$ all over the Fermi surface and δR_{\square} is in the tunnel regime. On the other hand, for a current in the [110] direction, δR_{\square} as a function of U_0 exhibits no features below $U_0 \approx \mu$ and is smaller than in the [100] case. For $U_0 > \mu$ the anisotropy vanishes. Numerical results for a barrier with $k_F d = 10^3$ where use is made of exact expressions for \mathcal{R} for a rectangular barrier are shown in Fig. 1. Note there is a kink in the [100] data at $U_0 = \mu/2$, as expected. The [110] data exhibit fast oscillations due to the oscillating behavior of \mathcal{R} at energies larger than U_0 . With increasing d the amplitude of the oscillations decreases since \mathcal{R} approaches a step function.

Temperature enters Eq. (4) via φ_0 . In Fig. 1, also δR_{\square} for a constant τ is shown. This is independent of the barrier direction and corresponds to the $T \rightarrow \infty$ limit of the cold-spot model. For $U_0 > \mu/2$ we thus find that δR_{\square} decreases with increasing T for the [100] barrier, whereas the reverse is true for the [110] case. Note that the T dependence of δR_{\square} is an analog of the violation of Mathiessen’s rule for additional

impurity scattering predicted^{7,5} for models with anisotropic τ . The latter has not been observed experimentally, however (see Ref. 5 for a discussion).

Discussion. Reference 5 ascribes Γ to scattering on superconducting fluctuations. An appealing alternative is to think of the hot segments as being insulating.²² A straightforward experimental test of this alternative is to study the anisotropy of tunneling ($T \rightarrow 0$). For tunneling in the [100] direction a nonvanishing current should be observed only for electrons leaving the high- T_c sample, while in the [110] direction standard metallic tunneling is expected for both signs of the current.

In a different class of theories, it is assumed that the normal state of the cuprates is dominated by fluctuating domain walls.²³ The local conductivity is, presumably, anisotropic. We expect that this scenario could be tested in a nonlinear conductivity experiment, but its analysis is beyond the scope of the present work.

In conclusion, we have studied direct experimental tests of the in-plane anisotropy of τ in the cuprates. We have shown that the magnetoresistance experiment is complicated by the not-well-understood c -axis velocity v_c . We have proposed nonlinear conductivity, skin effect, and transport across a barrier as experiments for the study of $\tau(\varphi)$. The magnitude of these effects within the cold-spot model has been estimated and the transport across a barrier seems to be most promising. A modification of the cold-spot model yielding magnetotransport in agreement with experiments has been proposed.

I thank V. Bezák, J. Foltin, and M. Grajcar for stimulating discussions. This work was supported by the Slovak Grant Agency Grant No. 1/4300/97 and the Comenius University Grant UK/3927/98.

APPENDIX

Standard transport theory⁸ for a tetragonal quasi-2D system with an arbitrary Fermi surface in a magnetic field in the z direction predicts

$$\begin{aligned} \sigma &= \sigma_0 \oint \frac{dk}{\pi} n_x^2 l, \\ \sigma_H &= -\sigma_0 \left(\frac{eB}{\hbar} \right) \oint \frac{dk}{\pi} n_x \frac{dn_y}{dk} l^2, \\ \Delta \sigma &= -\sigma_0 \left(\frac{eB}{\hbar} \right)^2 \oint \frac{dk}{\pi} \left[n_x^2 \left(\frac{dl}{dk} \right)^2 + \left(\frac{dn_x}{dk} \right)^2 l^2 \right], \end{aligned}$$

where l is the mean free path and n_a is the unit vector in the direction of the Fermi velocity. Integrals and derivatives are taken along the Fermi line. Let us assume now a modified cold-spot model with cold regions with a mean free path l_0 on portions δk of the Fermi line in the directions $[\pm 1, \pm 1]$. Moreover, let us assume that the local radius of curvature of the Fermi line in the cold spots is $\sim \delta k$. Then $\sigma_H \sim \sigma \Theta_H$ and $\Delta \sigma \sim \sigma \Theta_H^2$ with two independent quantities $\sigma \sim \sigma_0 \delta k l_0$ and $\Theta_H \sim eB l_0 / \hbar \delta k$, as in Anderson’s phenomenology.^{1,9} The magnetotransport data⁹ are reproduced with $l_0 \propto T^{-3/2}$ and $\delta k \propto T^{1/2}$. Assuming a Lorentzian

dependence of l around the cold spots, we predict $l \sim l_0(\delta k/k_F)^2 \propto T^{-1/2}$ in the hot regions of the Fermi line. Unfortunately, there is no evidence in photoemission experiments⁶ of a T -dependent Fermi line in the $[\pm 1, \pm 1]$ directions.

What could cause such a T dependence? In a system with broken particle-hole symmetry, $\delta\mu = \mu(T) - \mu(0) = -(\pi^2/6)T^2 N'(0)/N(0)$, where $N(0)$ and $N'(0)$ is the density of states and its derivative with respect to energy. If the Fermi line is defined as the locus of points where $\varepsilon_{\mathbf{k}} = \mu$, its shape (and volume) is T dependent in a system with anisotropic $v_{\mathbf{k}}$, since the shift of a point \mathbf{k} is $\delta\mu/\hbar v_{\mathbf{k}}$. However, from tunneling data²⁴ we estimate $N(0)/N'(0)$

≈ 1 eV for optimally doped BSCCO and therefore the expected shift of the Fermi line at $T=100$ K is only $\approx 10^{-4} \text{ \AA}^{-1}$.²⁵

On the other hand, there is a general argument showing the plausibility of a T -dependent Fermi line: We have postulated an angular dependence of the imaginary part Σ'' of the electron self-energy $\Sigma(\mathbf{k}, \omega)$. Fermi line is the locus of solutions of $\mu = \varepsilon_{\mathbf{k}}^0 + \Sigma'(\mathbf{k}, 0)$, where $\varepsilon_{\mathbf{k}}^0$ is the bare electron dispersion. Since Σ'' is T dependent and $\Sigma'(\mathbf{k}, 0) = (1/\pi) \int_{-\infty}^{\infty} d\omega \Sigma''(\mathbf{k}, \omega)/\omega$, we expect (for a system without particle-hole symmetry) an anisotropic T -dependent correction to the quasiparticle dispersion and hence a T -dependent Fermi line.²⁸

-
- ¹P. W. Anderson, Phys. Rev. Lett. **67**, 2092 (1991).
²D. K. K. Lee and P. A. Lee, J. Phys.: Condens. Matter **9**, 10 421 (1997).
³P. Coleman, A. J. Schofield, and A. M. Tsvelik, Phys. Rev. Lett. **76**, 1324 (1996).
⁴B. Stojković and D. Pines, Phys. Rev. B **55**, 8576 (1997).
⁵L. B. Ioffe and A. Millis, cond-mat/9801092 (unpublished).
⁶For a recent review, see M. Randeria and J. C. Campuzano, cond-mat/9709107 (unpublished).
⁷R. Hlubina and T. M. Rice, Phys. Rev. B **51**, 9253 (1995); **52**, 13 043(E) (1995).
⁸J. H. Ziman, *Electrons and Phonons* (Clarendon, Oxford, 1960).
⁹J. M. Harris *et al.*, Phys. Rev. Lett. **75**, 1391 (1995).
¹⁰A. S. Alexandrov, Phys. Rev. Lett. **79**, 4717 (1997).
¹¹N. E. Hussey *et al.*, Phys. Rev. Lett. **76**, 122 (1996).
¹²A. J. Schofield, J. R. Cooper, and J. M. Wheatley, cond-mat/9709167 (unpublished).
¹³T. Xiang and J. M. Wheatley, Phys. Rev. Lett. **77**, 4632 (1996).
¹⁴A. J. Millis *et al.*, cond-mat/9709222 (unpublished).
¹⁵J. Callaway, *Quantum Theory of the Solid State* (Academic, New York, 1974).
¹⁶For a review, see J. R. Cooper and J. W. Loram, J. Phys. I **6**, 2237 (1996).
¹⁷P. Böni *et al.*, Phys. Rev. B **38**, 185 (1988).
¹⁸The voltage jump on the barrier is generated by surface charges close to the barrier. The length scale on which the surface charge is substantial is given by the Thomas-Fermi screening length. In what follows, we include the surface-charge region as a part of the barrier. Therefore, the electric field outside the barrier can be taken constant.
¹⁹G. E. Blonder, M. Tinkham, and T. M. Klapwijk, Phys. Rev. B **25**, 4515 (1982).
²⁰Close to the barrier, the distribution functions for electrons moving away from the barrier differ from their bulk values. We neglect contributions to δR_{\square} which are due to spatial dependence of $f_{\mathbf{k}}$ in the electrodes.
²¹A barrier with a variable height can be realized, e.g., using a one-unit-cell-thick film of a high- T_c material covered by a thin insulating film, on top of which there is a metallic gate in the form of a thin stripe. Application of a finite voltage to the gate generates a potential barrier in the high- T_c film.
²²N. Furukawa and T. M. Rice, J. Phys.: Condens. Matter **10**, L381 (1998).
²³V. J. Emery, S. A. Kivelson, and O. Zachar, Phys. Rev. B **56**, 6120 (1997).
²⁴Ch. Renner *et al.*, Phys. Rev. Lett. **80**, 149 (1998).
²⁵Moreover, the jump of $d\mu/dT$ at T_c (which is a rough measure of $d\mu/dT$ in the normal state in a weak-coupling BCS treatment) is expected to change sign at optimal doping (Ref. 26). A similar sign change of $d\mu/dT$ has been found numerically in the t - J model (Ref. 27).
²⁶D. van der Marel and G. Rietveld, Phys. Rev. Lett. **69**, 2575 (1992).
²⁷J. Jaklič and P. Prelovšek, cond-mat/9803331 (unpublished).
²⁸Coupling-constant dependence of the Fermi line has been studied in A. V. Chubukov, D. K. Morr, and K. A. Shakhnovich, Philos. Mag. B **74**, 563 (1996).